

NamPRT and NNMT – key drivers of NAD-dependent signalling

Mathias Bockwoldt¹, Dorothée Houry², Marc Niere², Toni I. Gossmann³, Mathias Ziegler² and Ines Heiland^{1,§}

¹Department of Arctic and Marine Biology, UiT The Arctic University of Norway, Biologibygget, Framstredet 39, 9017 Tromsø, Norway

²Department of Molecular Biology, University of Bergen, Thormøhlensgt. 55, 5020 Bergen, Norway

³Department of Animal and Plant Sciences, Western Bank, University of Sheffield, Sheffield, S10 2TN, United Kingdom

§ Corresponding author: ines.heiland@uit.no

1 Summary

NAD is best known as cofactor in redox reactions, but it is also substrate of NAD-dependent signalling reactions that consume NAD and release nicotinamide (Nam). In eukaryotes, two different Nam salvage pathways exist. While in lower organisms the initial deamidation of Nam is prevalent, in animals the direct conversion of Nam to the mononucleotide by Nam phosphoribosyltransferase (NamPRT) dominates and eventually remains as the single Nam recycling route in vertebrates.

Strikingly, loss of the deamidation pathway in early vertebrates is preceded by the occurrence of a new enzyme that marks Nam for excretion by methylation – nicotinamide N-methyltransferase (NNMT). The physiological relevance of NNMT is still enigmatic. Why is there an enzyme that removes Nam from recycling, seemingly not having any other physiological role? And why is the occurrence of NNMT accompanied by a diversification of NAD-consuming enzymes?

We have used mathematical modelling approaches to resolve these counterintuitive observations. Our results indicate that NNMT is required to enable high NAD consumption fluxes necessitated by the increasing diversification of NAD-dependent signaling pathways. This kinetic regulation requires a high substrate affinity of the key enzyme for Nam salvage, NamPRT. Indeed, the affinity of NamPRT to Nam has previously been measured to be in the nanomolar range. Mathematical modelling supports the hypothesis that NNMT exerted an evolutionary pressure on NamPRT enforcing the development of its unusually high substrate affinity. Using multiple sequence alignments, we identified a sequence insertion, first occurring in vertebrates, that parallels an – experimentally verified – increase in the substrate affinity of the enzyme. Further simulations show that the deamidation pathway became obsolete owing to the high substrate affinity of NamPRT. Collectively, our results illustrate a close evolutionary relationship between NAD biosynthesis and the diversification NAD-dependent signalling pathways, potentially driven by the concomitant occurrence of a regulator of Nam salvage, NNMT.

2 Keywords

3 Introduction

NAD metabolism represents one of the most critical links that connect cellular signal transduction and energy metabolism. Even though best known as cofactor for various redox-reactions , NAD is involved in a number of signalling processes that consume NAD⁺ by cleaving the molecule to nicotinamide (Nam) and ADP-ribose [?]. These NAD⁺-dependent signalling reactions include but are not limited to poly- and mono-ADP-ribosylation, NAD⁺-dependent protein deacetylation by sirtuins as well as the synthesis of calcium mobilizing molecules such as cyclic ADP-ribose [?]. These NAD⁺-dependent signalling processes participate in the regulation of virtually all cellular activities. The enzymes involved in these processes are sensitive to the available NAD⁺ concentration [?], which in turn is dependent on the NAD⁺/NADH redox ratio. Therefore, NAD⁺-dependent signalling can act as a transmitter of changes in the cellular energy homeostasis, for example, to regulate gene expression or metabolic activity [?].

The significance of NAD⁺-dependent signalling for NAD homeostasis has long been underestimated. However, it has now been established that substances affecting NAD biosynthesis lead to a rapid decline of the NAD concentration [?] suggesting that NAD⁺-dependent signalling consumes substantial amounts of NAD, which is why we later refer to them also as NAD-consuming reactions. The resulting NAD turnover differs in a cell type specific manner and can lead to an NAD-halflife as short as 2 hours [?]. To maintain the NAD concentration at physiological levels, NAD biosynthesis needs to act at an equally rapid rate. Imbalances in NAD-homeostasis have been linked to various, in particular, ageing-related diseases such as diabetes, neurodegenerative disorders and cancer [?, ?]. Several recent studies have demonstrated impressive health benefits of dietary supplementation with intermediates of NAD biosynthesis including NMN and nicotinamide riboside, (NR) [?]. Apparently, the exploitation of NAD biosynthetic routes, in addition to the use of nicotinamide as precursor (Fig. 1), results in increased NAD concentrations that stimulate NAD⁺-dependent signalling processes, in particular, protein deacetylation by sirtuins [?].

Due to the constant release of Nam through NAD-consuming signalling reactions, the NAD salvage pathway using Nam as precursor is the most important NAD-synthesis pathway. If Nam would not be constantly recycled into NAD, humans would require a much higher daily vitamin B3 intake than the 16 mg that are the current daily recommendation [?]. In the first step of the salvage pathway, Nam is converted to the mononucleotide, NMN, by Nam phosphoribosyltransferase (NamPRT) using phosphoribosylpyrophosphate (PRPP) as co-substrate. The nearly complete recycling of Nam is achieved by an extraordinary high affinity of NamPRT to Nam, the Km being in the low nanomolar range [?]. Despite the importance of its salvage, Nam can also be marked for excretion by methylation. The presence of nicotinamide N-methyltransferase (NNMT) in vertebrates [?] is among the most enigmatic and counterintuitive features of NAD metabolism. Why is there one enzyme (NamPRT) seemingly optimized to recycle even the faintest amounts of Nam back into NAD synthesis, while at the same time there is another enzyme (NNMT) that seems to have no metabolic function other than to remove Nam from NAD metabolism, This puzzle becomes even more intriguing when considering that the majority of lower organisms and plants deamidated Nam to nicotinic acid (NA) using the nicotinamide deamidase (NADA) before it can enter NAD biosynthesis via

Mathias B.

Please add more references to the first paragraph. I think there are better references than my own review.

the Preiss-Handler pathway (Fig. 1).

We here present a phylogenetic analysis of NAD-pathway in eukaryotes that. In contrast to our previous analysis, which has been limited by the low number of eukaryotic genomes available at the time, we are now able to provide a comprehensively analysis of the eukaryotic pathway evolution. The results show there has seemingly been a selection for the co-existence of NamPRT and NNMT in Deuterostomia, while the pathway dominant in bacteria is lost. This was accompanied by a marked increase in the number of NAD+-consuming signalling enzymes. To explain these counterintuitive results we built a mathematical model of the pathway and demonstrated that NNMT has a critical role to maintain high NAD+-consuming signalling fluxes by preventing accumulation of inhibitory Nam. Our model furthermore predicts that NNMT likely exerted an evolutionary pressure on the NamPRT affinity development. Simulating the resource competition we furthermore show that the presence of high affinity NamPRT together with NNMT makes the NADA dependent pathway obsolete. Based on multiple sequence alignments, we identified a sequence insertion in NamPRT in Deuterostomes that is affecting the affinity of NamPRT, undermining the predictions derived from our mathematical modelling approach

Taken together, our analyses suggest that the co-existence of NamPRT and NNMT has been a prerequisite to enable the evolutionary development of versatile NAD+-dependent signalling mechanisms present in vertebrates.

4 Results

4.1 Phylogenetic analysis of NAD biosynthesis and consumption

NAD can be synthesized using several routes from three main precursors: tryptophan, nicotinamide (Nam) and nicotinic acid (NA) (Overview see Figure 1.). Nam and NA are together known as vitamin B3 or niacin. Alternatively, nicotinamide ribose (NR) can be used omitting the energetically unfavourable reaction of Nam phosphoribosyltransferase (NamPRT), requiring nicotinamide ribose kinase (NRK) instead [?]. Due to the high turnover of NAD observed and the fact that only 1% of the tryptophan taken up with our diet is converted into NAD, vitamin B3 (Nam and NA) and to a lower extend NR are the major precursor of human NAD-biosynthesis.

Looking across all known species, two different pathways exist that recycle NAM. The major pathway found in yeast and plants is using a four-step pathway starting with the deamination of Nam to nicotinic acid by NADA. The other three enzymes comprise the Preiss-Handler pathway that also exists in vertebrates. The recycling pathway found in mammals directly converts Nam into the corresponding mononucleotide (NMN) a reaction catalysed by NamPRT and driven by a non-stoichiometric ATP-hydrolysis. A similar reaction catalysed by an evolutionary related enzyme NAPRT, converts NA into the NA mononucleotide in the Preiss-Handler pathway. NMN and NAMN are converted into dinucleotides by the Nam/NA adenylyltransferases (NMNATs). The recycling pathway via NA finally requires an amidation step catalysed by NADsynthase, driven by the conversion of ATP to AMP producing pyrophosphate. Even though the latter pathway seems to be very inefficient, it is the pathway preferentially used by most bacteria, fungi and plants (see Figure 2A), whereas most metazoans recycle Nam using NamPRT.

Analysing the phylogeny of the NAD recycling enzymes in Metazoa in more detail reveals that not only does NamPRT replace NADA, but in most organisms, espe-

cially in Deuterostomia, NamPRT is found together with the Nam methyltransferase NNMT (Figure 2B). NNMT methylates Nam to methyl-Nam that is in mammals excreted with the urine, thus removing Nam from recycling. NNMT seems to have arisen de novo in the common ancestor of Ecdysozoa and Lophotrochozoa. We were not be able to find any gene with considerable similarity in fungi or plants, even though in fungi a genes named NNMT can be found in databases. These genes do, however, show very limited sequence similarities to the NNMT of nematodes or deuterostomes and the yeast protein has later on shown to be a lysin-protein-methyltransferase [?]. Nematodes are the only organisms that encode NNMT together with NADA without NamPRT being present. In Deuterostomia the only large class that does only have NamPRT and seems to have lost NNMT again are Sauropsida and here especially birds. The reason why a lot of birds do not encode NNMT remains unclear, as the appearance is quite scattered (not shown). It might be related to the excretion system, as the product of NNMT methyl-nicotinamide is in mammals excreted with the urine. There are some species where we could not find NamPRT or NADA but NNMT, we assume that this is due to incomplete genomes in the database.

In addition to the phylogenetic distribution of the two Nam salvage enzymes NADA and NamPRT, we looked at phylogenetic diversity of enzymes catalysing NAD-dependent signalling reactions. To do so we used the previously established classification into 10 different enzyme families [?]. The detailed list of templates used for the phylogenetic analysis can be found in Supplementary Table 1 . The numbers in Figure 2B denote the average number of NAD-dependent signalling enzyme families found in each taxa. With the exception of Cnidaria and Lophotrochozoa, we find average 3 to 4 families in Protostomia, whereas most Deuterostomia have on average more than 8 families with an increasing diversification of enzymes within some of these families [?].

Taken together, we found that the presence of NamPRT and NNMT coincides with an increased diversification of NAD-dependent signalling, whilst NADA is lost in vertebrates. This seems counterintuitive, as one would expect that a decrease in precursor concentration caused by the precursor removal through NNMT, should cause a decrease of NAD availability and consequently less active NAD dependent signalling.

4.2 Dynamics of NAD biosynthesis and consumption

So why does the diversity of NAD-dependent signalling increase? And why does NADA disappear in Deuterostomia although it is the predominant pathway in bacteria, plants and fungi? Given the complexity of the NAD metabolic network, this questions are difficult to be comprehensively addressed experimentally. We therefore built a dynamic model of NAD metabolism using existing kinetic data from the literature (for details see materials and methods and supplementary table 2).

To be able to compare metabolic features of evolutionary quite different systems in our simulations, and as we have limited information about expression levels of enzymes or changes of kinetic constants during evolution, we initially used the kinetic constants found for yeast or human enzymes for all systems analysed and used equal amounts of enzymes for all reactions. Wherever possible we did not only include substrate affinities but also known product inhibition or inhibition by downstream metabolites. As we assume that cell growth is, besides NAD-consuming reactions, a major driving force for NAD biosynthesis, we analysed different growth rates (cell

Mathias
Maybe as supplementary figure?

Mathias
Include number and order and name Supplementary Tables accordingly

division rates) by simulating different dilution rates for all metabolites.

First we addressed the question of the predominant co-existence of NamPRT and NNMT in vertebrates that coincides with an increase in the number of NAD-consuming enzyme families. We thus used our dynamic model to simulate steady state concentrations and NAD-consumption rates simulating NAD biosynthesis via NamPRT in the presence or absence of NNMT. We see that the presence of NNMT enables higher NAD consumption rates (Figure 3A) while, as expected, reducing the steady state concentration of NAD (Figure 3B). The decline in NAD-concentration can be compensated by a higher expression of NamPRT further increasing NAD consumption flux (Figure 3A and B dashed lines).

These findings can be explained when looking in more detail at the kinetic parameters of NamPRT and NAD-consuming enzymes such as Sirt1p. The increase of NAD consumption flux is caused by the fact that most NAD-consuming enzymes are inhibited by their product Nam, explaining why the presence of NNMT enables higher NAD consumption fluxes. At the same time, the high substrate affinity of NamPRT maintains a sufficiently high NAD-concentration.

As kinetic parameters of NamPRT are only available for the human enzyme [?], we went on to theoretically analysed the potential effect of the NamPRT affinity (K_M) on NAD steady state concentration and NAD consumption flux. In the absence of NNMT (Figure 4A-B) a change in K_M has very little effect on steady state NAD concentration and NAD consumption flux. In the presence of NNMT, however, NAD consumption flux and NAD concentration increases with decreasing K_M values (Figure 4C-D).

It is interesting to note that, without NNMT, NAD concentration and consumption flux are both considerably affected by cell division rates, at least if the enzyme expression is kept constant. This is of course an artificial scenario, as one would assume organisms to regulate enzyme expression to achieve similar levels of metabolite concentrations instead. However, there seems to be an apparent trade off between maintainable NAD concentration and consumption flux in the absence of NNMT. In contrast, NAD consumption rates increase with NAD concentration in the presence of NNMT and both are relatively independent of cell division rates.

When we compare NAD consumption and NAD concentration with and without NNMT with two different substrate affinities of NamPRT, we see that at low affinity (K_M of 1 μ M, which is in the range of the K_M of NADA for Nam), NAD consumption flux is only higher with NNMT at low cell division rates. This effect becomes stronger with decreasing affinity (Figure 4E-F).

The pathway dynamics are of course not solely dependent on one enzyme. Thus, what is the impact of the substrate affinity of NNMT that is competing with NamPRT for the same substrate? In Figure 5 we see that the substrate affinity values found in the human enzymes (indicated by black asterisks) are actually optimal with respect to both achievable steady state NAD concentration and consumption fluxes. Thus, a further increase of the affinity of NamPRT for Nam would not provide any advantage.

4.3 Sequence variance acquired in metazoans enhances substrate affinity

As our simulations suggest that NNMT might have exerted an evolutionary pressure on the development of NamPRT. We performed multiple sequence analysis to see if we can find sequence variations in the protein sequence of NamPRT that indi-

cate evolutionary changes of NamPRT upon the appearance of NNMT. The multiple sequence alignment of selected sequences is shown in Figure 5A and a more comprehensive multiple sequence alignment containing a larger number of species can be found in Supplementary Figure 1. We recognized that most Deuterostomia that have only NamPRT and NNMT (indicated by the blue circle) have an insert of ten amino acids corresponding to positions 43 to 52 of the human enzyme. This insert overlaps with a predicted weak nuclear localisation signal, that is lost when removing this sequence stretch. The inserted sequence corresponds to a structurally unresolved loop in all available crystal structure of human NamPR (e.g. [?] structure visualisation Figure 5B). The loop is connected to one of the beta-sheets involved in substrate binding.

From these observations we derived two possible hypotheses regarding the role of the loop for NamPRT function. Firstly, we analysed whether the deletion of the amino acids 42 to 51 has an effect on the localisation of the human enzyme. We thus performed immunofluorescence imaging with FLAG-tagged proteins, but both wildtype and mutant protein showed a mixed cytosolic nuclear localisation (Figure 6C). We therefore conclude that the partial nuclear localisation of NamPRT is not affected by the sequence deletion. The second hypothesis was that the sequence insertion influences NamPRT affinity, which is what our mathematical simulations would predict. We thus recombinantly expressed both wildtype and mutant NamPRT in *E. coli*. Upon purification we measured the activity using NMR detection of NMN produced in the presence and absence of ATP. It appears that the enzymatic activity of the mutant enzyme is much lower than that of the wildtype enzyme (Figure 6D) and that an increase of the substrate concentration has a much stronger effect on the activity of the mutant compared to the wildtype enzyme, indicating a lower affinity. We furthermore showed that in contrast to NamPRT wildtype, the mutant does not exhibit an increased activity in the presence of ATP (Figure 6E).

4.4 Loss of NADA in vertebrates

The remaining question is now, why NADA is lost in vertebrates, while NADA and NamPRT are co-existing in bacteria? To analyse this question we built a two compartment model that has a shared Nam source (details see Materials and Methods and Supplementary Material). One compartment contains NADA while the other contains either NamPRT alone at equal expression levels, or together with NNMT. Without NNMT the compartment containing NADA has slightly lower NAD consumption rates (Figure 7A), but is able to maintain much higher steady state NAD concentrations at low cell division rates (Figure 7B). At high cell division rates, steady state concentrations in both compartments are similar. The latter might explain why in bacteria that have relatively high growth rates both systems co-exist. In the presence of NNMT the NamPRT compartment out-competes the NADA containing compartment, both with respect to NAD consumption rates and steady state NAD concentrations (Figure 7 C and D). This effect is dependent on a high affinity of NamPRT, as at low affinity (high K_M) the NADA containing system is again able to maintain higher NAD-concentrations. The NAD consumption flux is still higher in the NamPRT and NNMT containing compartment. Taken together this might explain why upon the development of a sufficiently high affinity of NamPRT for its substrate, which seems to have been induced by the appearance of NNMT, NADA is lost.

5 Discussion

The dynamic interactions among metabolism, signal transduction, and gene regulation is still not very well understood. New approaches are required to disentangle the underlying network, helping us to understand how alterations affect human physiology. We here combined phylogenetic analysis and mathematical modelling the NAD biosynthesis and consumption pathway to better understand the evolution of this pathway and especially the role of the methyltransferase NNMT. Our analysis reveals that NNMT plays a vital role for the diversification of NAD-dependent signalling reactions and potentially also for NAD homeostasis. We show that the presence of NNMT enables higher NAD consumption rates in comparison to NamPRT or NADA alone. It furthermore appears that NNMT makes both NAD concentration and NAD consumption relatively independent of other NAD requiring processes such as cell growth. We furthermore suggest that NNMT exerted an evolutionary pressure on NamPRT driving the development of the high affinity of NamPRT for its substrates found in the human enzyme [?]. These findings shed new light on the role of NNMT, which has earlier been recognized as potential marker for some types of cancer (e.g. [?]), hinting that increased NNMT expression in cancer might serve to remove NAM produced by increased NAD-dependent signalling. Further analysis is required to better understand which NAD-signalling reactions are affected. But given a better mechanistic understanding and as routine clinical measurements of urine methyl-Nam (MNam) concentrations are available already, MNam could potentially serve as biomarker in the context of different diseases (e.g[?, ?]).

In our analysis we furthermore noted that NNMT only provides an advantage as long as the NamPRT affinity for Nam is sufficiently high, this implies that treatment with competitive inhibitors that affect the apparent K_M would have stronger effects on cells that express NNMT compared to cells that don't express NNMT (see Figure 4E-F). This could be important for cancer treatments as the expression of NNMT is relatively low in normal tissues except liver, whereas several types of cancer overexpress NNMT.

We here neglected the potential effects of the methyl donor S-adenosyl-methionine (SAM) and its precursor methionine, although it is most likely contributing yet another regulatory level for Nam availability and thus an additional interaction point between gene regulation and metabolism. It has been shown earlier that NNMT expression influences protein methylation dependent on methionine availability [?]. One of the challenges in the analysis of this aspect is the availability of *in vivo* concentration measurements for SAM and the large amount of reactions using it as substrate. A mathematical model of this pathway has recently been published that could provide the basis for further studies.

6 Conclusions

Beside the evolutionary changes analysed here we have detected further evolutionary events in the development of NAD biosynthesis. We noted for example that the unresolved loop insertion in NamPRT co-appears together with the first gene duplication of the NMNAT and thus the development of NMNAT2 [?]. At the point of the second gene duplication of NMNAT and thus the development of NNMT3 coincides with a positive selection event in NNMT (overview Figure 8).

I think we should leave this for a later manuscript

7 Experimental Procedure

7.1 Dynamic modelling

Kinetic parameters (substrate affinity (K_m) and turnover rates (k_{cat}), substrate and product inhibitions) were retrieved from the enzyme database BRENDA and additionally evaluated by checking the original literature especially with respect to measurement conditions. Parameter values from mammals were used if available. For enzymes not present in mammals, values from yeast were used. The full list of kinetic parameters including reference to original literature can be found in Supplementary table 1. For NMNAT, the previously developed rate law for substrate competition was used [?]. Despite these modifications, Henri-Michaelis-Menten kinetics were used for all reactions except the import and efflux of Nam, which were simulated using constant flux and mass action kinetics, respectively. All simulations were performed using the steady state calculation and parameter scan options provided by COPASI 4.22 [?]. The model will be available at the Biomodels database accession number xxx. Related figures were generated using gnuplot.

Ines

Insert number

7.2 Phylogenetic Analysis

NADA, NamPRT, and NNMT enzymes or enzyme candidates were identified using Blastp with known enzymes against the NCBI non-redundant protein sequence database (nr). A list of functionally verified enzymes used as templates is given in supplementary table 2. This table also includes the length cut-offs for identified enzymes. The e-value cut-off was 1e-30 for all enzymes. Blastp parameters were set to yield maximum 20 000 target sequences, using the BLOSUM62 matrix with a word size of 6 and gap opening and extension costs of 11 and 1, respectively. Low-complexity filtering was disabled. Obvious sequence contaminations were removed by manual inspection of the results. The taxonomy IDs of the species for each enzyme was derived from the accession2taxon database provided by NCBI. Scripts for creating, analysing, and visualising the phylogenetic tree were written in Python, using the ETE3 toolkit (Huerta-Cepas, 2010).

Ines

Version?

7.3 Generation of expression vectors encoding wild-type and mutant human NamPRT

For eukaryotic expression with a C-terminal FLAG-epitope, the open reading frame (ORF) encoding human NamPT was inserted into pFLAG-CMV-5a (Merck - Sigma Aldrich) via EcoRI/BamHI sites. Using a PCR-based approach, this vector provided the basis for the generation of a plasmid encoding a NamPT deletion mutant lacking amino acid residues 42-51 (NamPT- Δ 42-51). For prokaryotic expression with an N-terminal 6xHis-tag, the wild-type and mutant ORFs were inserted into pQE-30 (Qiagen) via BamHI and PstI-sites. All cloned sequences were verified by DNA sequence analysis.

7.4 Transient transfection, immunocytochemistry, and confocal laser scanning microscopy

HeLa S3 cells cultivated in Ham's F12 medium supplemented with 10% (v/v) FCS, 2 mM L-glutamine, and penicillin/streptomycin, were seeded on cover slips in a 24

well plate. After one day, cells were transfected using Effectene transfection reagent (Qiagen) according to the manufacturer's recommendations. Cells were fixed with 4% paraformaldehyde in PBS 24 hours post transfection, permeabilised (0.5% (v/v) Triton X-100 in PBS) and blocked for one hour with complete culture medium. After overnight incubation with primary FLAG antibody (mouse M2, Sigma-Aldrich) diluted 1:2500 in complete medium, cells were washed and incubated for one hour with secondary AlexaFluor 594-conjugated goat anti mouse antibody (ThermoFisher, Invitrogen) diluted 1:1000 in complete culture medium. Nuclei were stained with DAPI and the cells washed. The cover slips were mounted on microscope slides using Pro-Long Gold (ThermoFisher, Invitrogen). Confocal laser scan imaging of cells was performed using a Leica TCS SP8 STED 3x microscope equipped with a 100x oil immersion objective (numerical aperture 1.4).

7.5 Purification of NamPRT

The cells were harvested by centrifugation and resuspended in lysis buffer (20 mM Tris-HCl pH 8.0, 500 mM NaCl, 4 mM dithiothreitol (DTT), 1 mg/mL lysozyme, 1X Complete EDTA-free protease inhibitor cocktail (Roche)). After sonification, the lysate was centrifuged for 30 min at 13000 g, and the clear lysate was incubated with 2 mL of Nickel-NTA resin (Qiagen). Non-specific protein binding was removed with washing buffer (20 mM Tris-HCl pH 8.0, 500 mM NaCl, 1 mM DTT, 20 mM imidazole). The protein was eluted with 2.5 mL of elution buffer (20 mM Tris-HCl pH 8.0, 500 mM NaCl, 300 mM imidazole).

The eluted protein was immediately subjected to size exclusion chromatography (SEC) on an ÄKTA pure system (GE Healthcare) and loaded onto a HiLoad 16/60 Superdex 200 pg column (GE Healthcare), run at a flow rate of 1 mL/min with SEC buffer (20 mM Tris-HCl pH 8.0, 500 mM NaCl). Fractions corresponding to the size of recombinant protein were pooled and used for enzymatic assay. The purity and size of the protein were assessed by SDS-PAGE.

7.6 Enzymatic Assay

2 µM of enzyme were incubated with 5-phospho-D-ribose 1-diphosphate (PRPP, 0.1 mM or 1 mM) and nicotinamide (Nam, 0.1 mM or 1 mM) in reaction buffer (20 mM Tris-HCl pH 8.0, 500 mM NaCl, 2 mM MgCl₂, and 0.03% BSA), in absence or presence of 1 mM of adenosine triphosphate (ATP). The 1.2 mL reaction was incubated for 10 minutes at 30 °C and the enzymatic activity stopped with 0.1 mM of FK866, the samples were frozen in liquid nitrogen.

7.7 Sample preparation and NMR spectroscopy

The samples were dried with an Eppendorf Vacufuge Concentrator, and then resuspended with 200 µl of NMR buffer containing 5% deuterated H₂O (D₂O) and 1 mM 4,4-dimethyl-4-silapentane-1-sulfonate (DSS).

1D ¹H NMR spectra were acquired on a 850 MHz Ascend Bruker spectrometer equipped with 5 mm TCI triple-resonance CryoProbe and a pulse field gradients along the z-axis. The experiments were acquired with zgsgpppe pulse sequence, allowing water suppression using excitation sculpting with gradients and perfect echo. The temperature was kept constant at 300 K and the acquisition parameters were the following: number of scans = 2000, relaxation delay = 1 s, acquisition time = 1.6 s, data points = 65K, and spectral width = 14 ppm.

The spectra phase and baseline were automatically and manually corrected using TopSpin 3.5 software (Bruker Biospin). Quantification of nicotinamide mononucleotide (NMN) was done by the integration of the peak at 9.57 ppm and DSS used as an internal standard.

8 Figure Legends

8.1 Figure 1

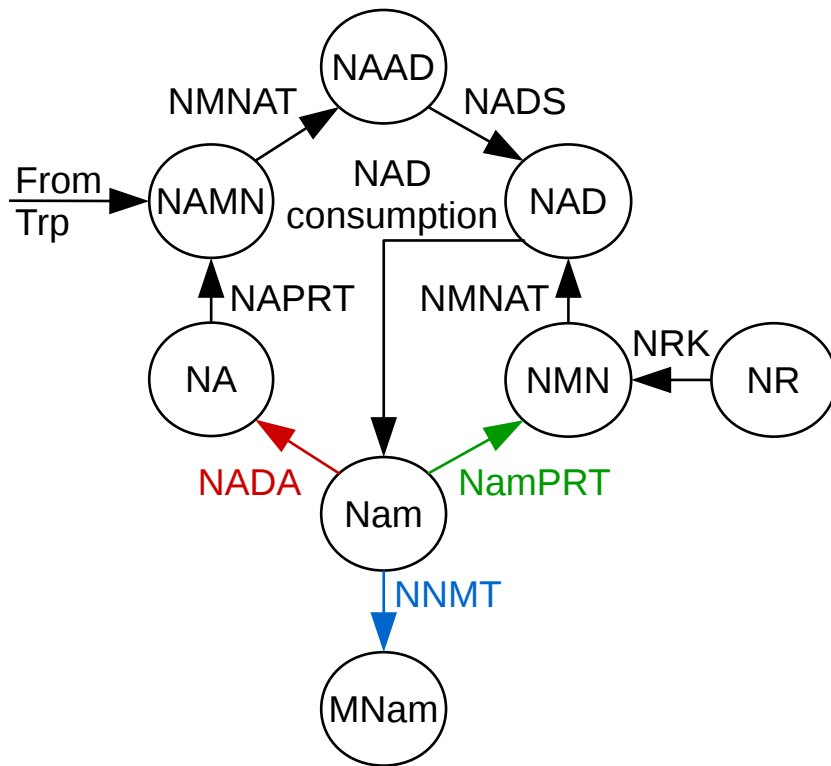


Figure 1: **Schematic overview of NAD biosynthesis and consumption.** NAD can be synthesized from tryptophan (Trp), nicotinamide (Nam), nicotinic acid (NA), and, to a lesser extend, nicotinamide ribose (NR). Nam is the main precursor and also the product of NAD-consuming signalling reactions by enzymes such as sirtuins (NAD-dependent histone deacetylases) or PARPs (poly-ADP-ribosylases). For the recycling of Nam, two different pathways exist. The pathway found in yeast and many bacteria starts with the deamination of Nam by Nam deamidase (NADA). The other three enzymes comprise the Preiss-Handler pathway that also exists in vertebrates. The pathway found in vertebrates directly converts Nam into the corresponding mononucleotide (NMN) by the Nam phosphoribosyltransferase (NamPRT). A third enzyme can consume Nam, the Nam N-methyltransferase (NNMT). For more details and abbreviations, see text.

8.2 Figure 2

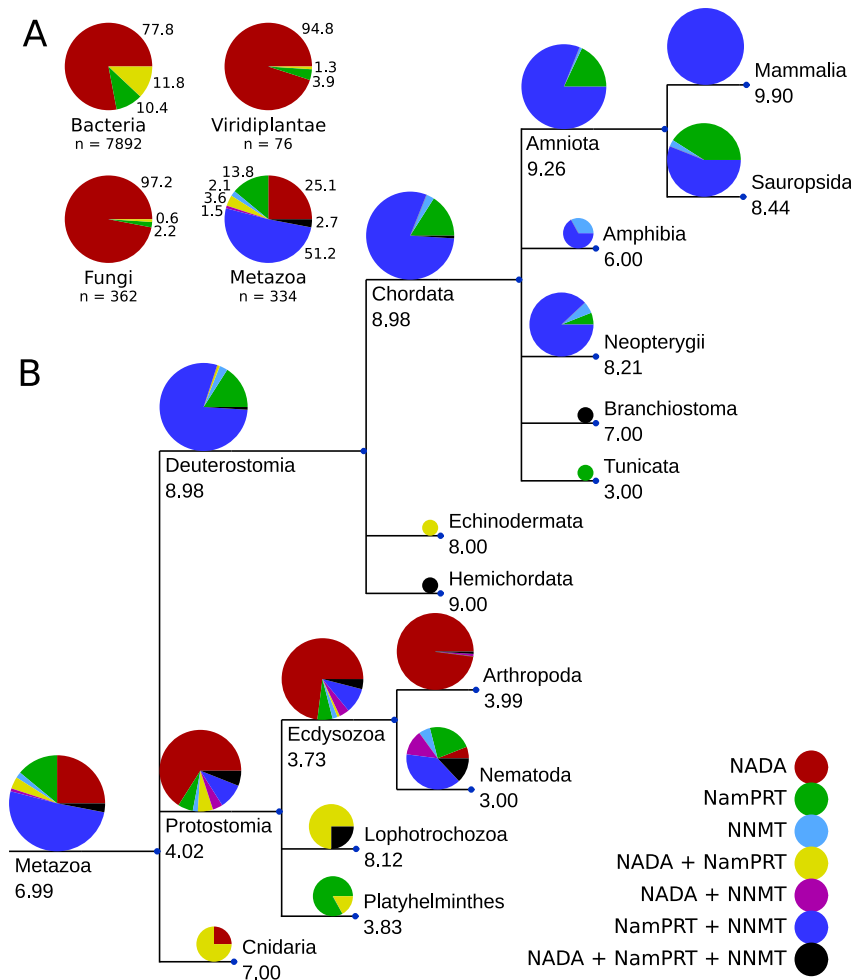


Figure 2: **Evolutionary distribution of NADA, NNMT and NamPRT and their relation to the number of NAD consumers.** A) Distribution of NADA, NNMT and NamPRT in selected major taxa. NADA is dominant in Bacteria, Fungi, and Plants (Viridiplantae), whereas NamPRT together with NNMT is dominant in Metazoa. Numbers at the pie charts show, how many species of the taxon possess the respective enzyme combination indicated by the colour explained in the lower right of the figure. Below the taxon name, the number of species in that taxon is given. B) Common tree of selected taxa within the Metazoa, including 334 species. The pie charts indicate the distribution of species within the respective taxon that have the enzyme combination indicated by the colour explained in the lower right. The size of the pie charts is proportional to the logarithm of the number of species analysed in the particular taxon. The numbers below the taxon names indicate the average number of NAD-consuming enzyme families found in all sub-taxa. The branch length is arbitrary.

8.3 Figure 3

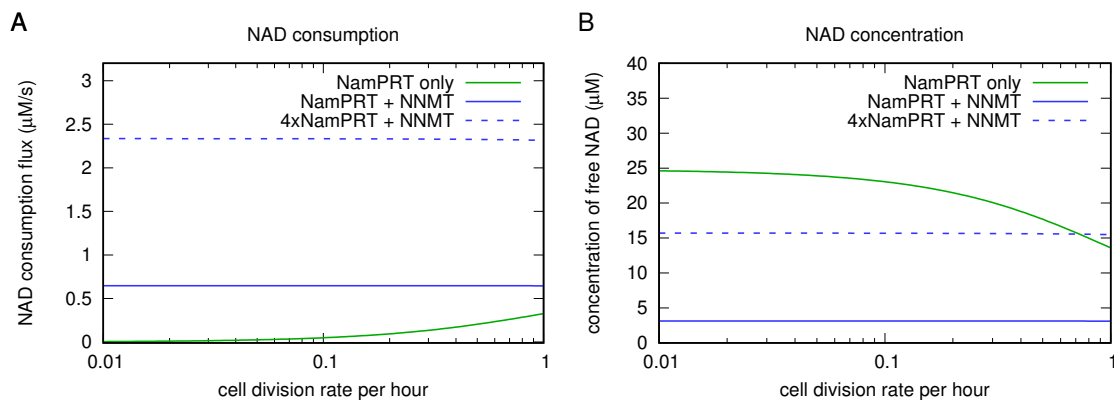


Figure 3: **NMMT enables high NAD-consumption flux.** We used a dynamic model of NAD biosynthesis and consumption (details see Materials and Methods) to simulate NAD consumption flux (A) and NAD concentration (B) in the presence of NamPRT and with or without NMMT at different cell division rates. NMMT enables higher steady-state NAD consumption flux despite reduced NAD concentrations.

8.4 Figure 4

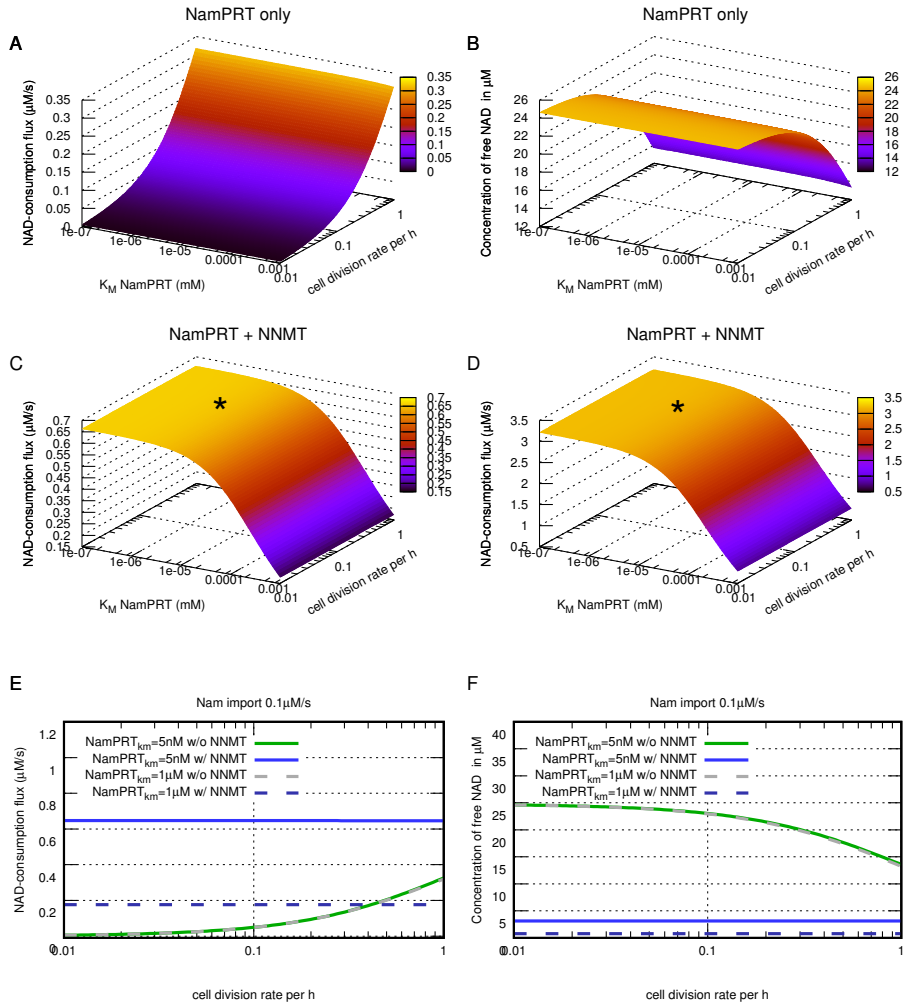


Figure 4: Role of NamPRT affinity for Nam. Using the dynamic model of NAD biosynthesis and consumption we simulated the affect of different Michaelis Menten constants (K_M) of NamPRT for Nam on steady-state NAD consumption flux and NAD concentration at different cell devision rates. In the absence of NNMT (A and B), the K_M of NamPRT has little influence on NAD consumption and concentration, but both are changing with cell devision rates. In the presence of NNMT (C and D), decreasing K_M of NamPRT enables increasing NAD consumption flux and NAD concentration. NNMT furthermore makes both, consumption flux and concentration, relatively independent of cell division rates. Comparing the situation with and without NNMT (E and F) at different NamPRT K_M reveals that at low K_M and high cell devision rates NNMT no longer enables higher NAD consumption rates compared to NamPRT alone.

8.5 Figure 5

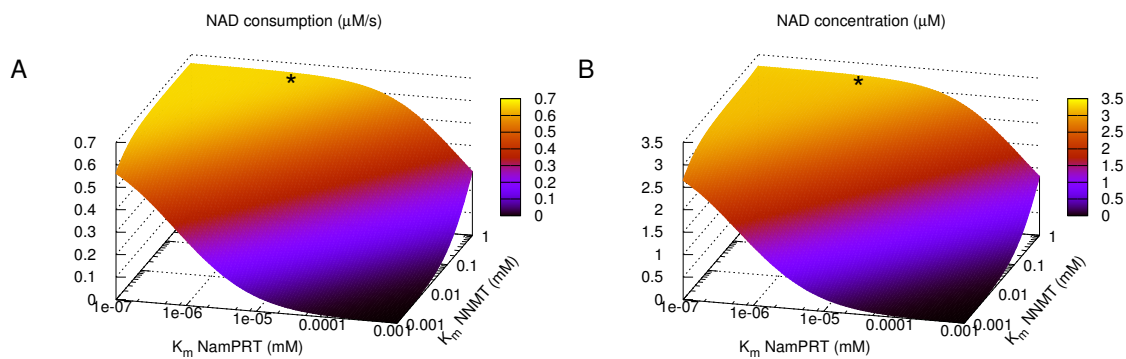


Figure 5: **The substrate affinities of human NNMT and NamPRT are optimal.** Both NAD consumption flux (A) and NAD concentration (B) are increasing with decreasing K_M of NamPRT but decreasing K_M of NNMT. The affinities reported for human enzymes (indicated by a black asterisk) appear to be close to optimal, as further improvements would have little or no effect on NAD consumption or concentration.

8.6 Figure 6

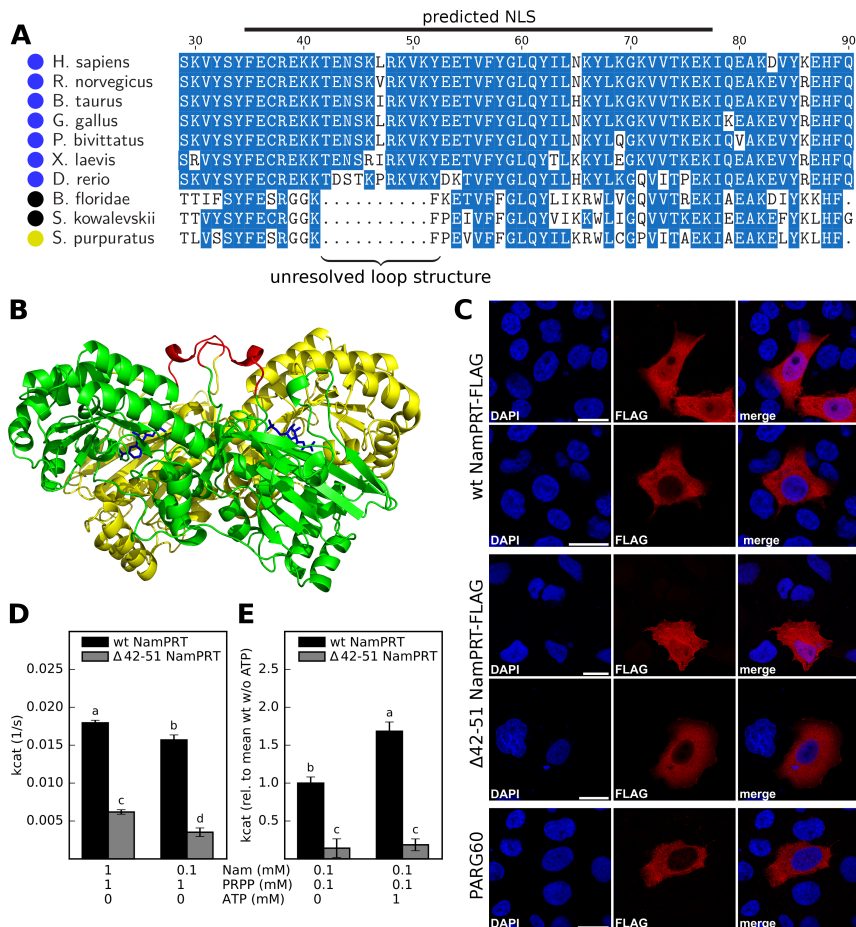


Figure 6: The function of the structurally unresolved loop structure of NamPRT. Most Deuterostomia that encode NNMT show a sequence insertion in the N-terminal region of NamPRT that has been revealed by multiple sequence alignment of NamPRT from different species (A). Coloured circles indicate the enzymes present in the species besides NamPRT; blue: NNMT; black: NADA and NNMT; yellow: NADA. For a more comprehensive alignment, please see supplementary figure S1. B) The visualisation of human NamPRT is based on a structure prediction of SWISS-MODEL [?, ?] of the sequence of the human NamPRT using the model 2H3D as template [?]. The inserted region is not resolved in crystal structures of NamPRT and thus appears to be a flexible loop structure at the surface of the NamPRT dimer, coloured in red. C) The localisation of the FLAG-tagged mutant protein lacking the unresolved loop is not changed compared to wildtype human NamPRT. Both show a heterogenous nuclear cytosolic localisation in immunofluorescence images in HeLa S3 cells. But *in vitro* measurements show that the mutant NamPRT has lower activity than the wildtype enzyme (D) and is not activated by ATP (E). Bars in D) and E) with different letters indicate significant difference as estimated with a T test assuming independent samples and significance at $p < 0.05$.

8.7 Figure 7

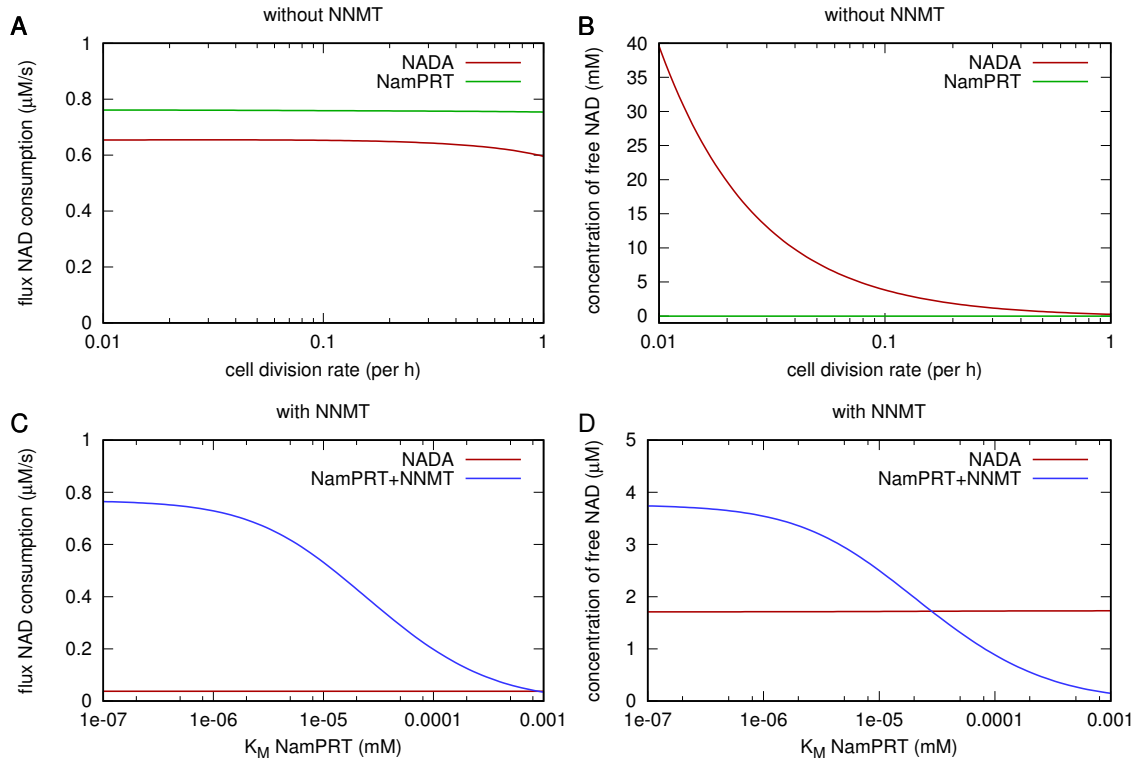


Figure 7: NNMT provides a competitive advantage and makes NADA obsolete. To simulate competition for common resources, we created a two compartment model where one compartment contained NADA but no NamPRT and the other compartment contained NamPRT either with or without NNMT but no NADA. In the absence of NNMT (A and B) the compartment containing NADA has slightly lower NAD consumption rates (A) but much higher NAD concentrations (B). In the presence of NNMT, however, both NAD consumption (C) and NAD concentration (D) are lower in the NADA compartment, but this effect is only observed at low NamPRT K_M .

9 Supplementary Legends

9.1 Supplementary figure S1

The structurally unresolved loop structure of NamPRT. Sequence alignment of NamPRT of different species cropped to the region around the unresolved loop structure. Coloured rectangles indicate the enzymes present in the species besides NamPRT; blue: NNMT; black: NADA and NNMT; yellow: NADA; green: NamPRT only. Major clades are indicated for better orientation. Number of amino acid indicated at the top refer to the human protein.

9.2 Supplementary figure S2

Distribution of NNMT in birds. ...

Figure must be made!

9.3 Supplementary table S1

Overview of kinetic constants used for the construction of the model.

9.4 Supplementary table S2

Query proteins used for Blast searches.